AIP Applied Physics Letters

Suppression of 1/f noise in near-ballistic h-BN-graphene-h-BN heterostructure field-effect transistors

Maxim A. Stolyarov, Guanxiong Liu, Sergey L. Rumyantsev, Michael Shur, and Alexander A. Balandin

Citation: Applied Physics Letters **107**, 023106 (2015); doi: 10.1063/1.4926872
View online: http://dx.doi.org/10.1063/1.4926872
View Table of Contents: http://scitation.aip.org/content/aip/journal/apl/107/2?ver=pdfcov
Published by the AIP Publishing

Articles you may be interested in

Microscopic origin of low frequency noise in MoS2 field-effect transistors
APL Mat. **2**, 092515 (2014); 10.1063/1.4895955

Large on/off current ratio in hybrid graphene/BN nanoribbons by transverse electric field-induced control of bandgap
Appl. Phys. Lett. **105**, 073114 (2014); 10.1063/1.4893697

Graphene-GaAs/ Al x Ga 1 − x As heterostructure dual-function field-effect transistor
Appl. Phys. Lett. **101**, 202104 (2012); 10.1063/1.4767387

Tunneling mechanism of the 1∕f noise in GaN∕AlGaN heterojunction field-effect transistors
J. Appl. Phys. **97**, 123706 (2005); 10.1063/1.1931033

1∕f noise in Ga N∕Al Ga N heterostructure field-effect transistors in high magnetic fields at 300 K
J. Appl. Phys. **96**, 3845 (2004); 10.1063/1.1787911

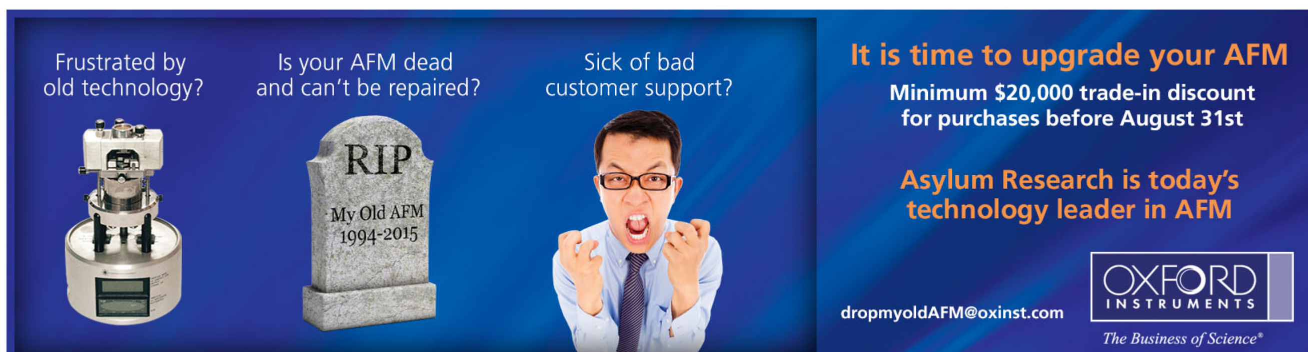

This article is copyrighted as indicated in the article. Reuse of AIP content is subject to the terms at: http://scitation.aip.org/termsconditions. Downloaded to IP: 172.15.52.34 On: Tue, 14 Jul 2015 15:28:10

APPLIED PHYSICS LETTERS **107**, 023106 (2015)

Suppression of 1/*f* noise in near-ballistic *h*-BN-graphene-*h*-BN heterostructure field-effect transistors

Maxim A. Stolyarov,[1] Guanxiong Liu,[1] Sergey L. Rumyantsev,[2,3] Michael Shur,[2] and Alexander A. Balandin[1,a)]

[1]*Nano-Device Laboratory (NDL) and Phonon Optimized Engineered Materials (POEM) Center, Department of Electrical and Computer Engineering, Bourns College of Engineering, University of California – Riverside, Riverside, California 92521, USA*

[2]*Departments of Electrical, Computer and Systems Engineering and Physics, Applied Physics, and Astronomy, Rensselaer Polytechnic Institute, Troy, New York 12180, USA*

[3]*Ioffe Physical-Technical Institute, Russian Academy of Sciences, St. Petersburg 194021, Russia*

(Received 12 June 2015; accepted 4 July 2015; published online 14 July 2015)

We have investigated low-frequency 1/*f* noise in the boron nitride–graphene–boron nitride heterostructure field-effect transistors on Si/SiO_2 substrates (*f* is a frequency). The device channel was implemented with a single layer graphene encased between two layers of hexagonal boron nitride. The transistors had the charge carrier mobility in the range from ~30 000 to ~36 000 cm^2/Vs at room temperature. It was established that the noise spectral density normalized to the channel area in such devices can be suppressed to $\sim 5 \times 10^{-9}\,\mu\mathrm{m}^2\,\mathrm{Hz}^{-1}$, which is a factor of $\times 5 - \times 10$ lower than that in non-encapsulated graphene devices on Si/SiO_2. The physical mechanism of noise suppression was attributed to screening of the charge carriers in the channel from traps in SiO_2 gate dielectric and surface defects. The obtained results are important for the electronic and optoelectronic applications of graphene. © *2015 AIP Publishing LLC*.
[http://dx.doi.org/10.1063/1.4926872]

The most realistic of the proposed electronic applications of graphene are those that do not seriously suffer from the absence of an energy bandgap but rely mostly on graphene's high electron mobility, thermal conductivity, saturation velocity, and a possibility of tuning the charge carrier concentration over a wide range.[1,2] These applications are in analog electronics,[3–5] high-frequency graphene devices for communications,[6,7] and terahertz plasmonic devices,[8,9] which benefit from graphene's excellent electron mobility and saturation velocity, as well as in chemical and biological sensing enabled by the ultimately high surface-to-volume ratio and the precise control of the carrier concentration.[10–13] For all these applications, the low-frequency electronic 1/*f* noise is a crucial performance metric (here *f* is the frequency). The low-frequency noise, usually found at frequencies below 100 kHz, limits the sensitivity and selectivity of all the sensors that rely on an electrical response. It is also responsible for the dominant contribution to the phase noise of the communication systems even when they operate at much higher carrier frequency.[14–16] From the fundamental physics point of view, graphene, as a truly two-dimensional material system, presents an interesting testing ground for theories describing the origin and mechanisms of 1/*f* noise.[17–19]

Owing to the importance of the subject, there have been numerous reports on 1/*f* noise in graphene devices.[17–30] Despite some data scatter due to unavoidable differences in graphene and device quality, most of the studies agree on the following characteristics of low-frequency noise in graphene. The low-frequency noise spectral density, S_I, in graphene devices is proportional to I^2 (here I is the drain–source current). The latter implies that the electrical current does not drive the fluctuations but merely makes them visible as in other homogeneous conductors.[31] Although both the graphene layer itself and metal contacts contribute to the 1/*f* noise, the dominant contribution mostly comes from the graphene channel itself. The results obtained by different groups for micrometer size graphene devices on Si/SiO_2 substrates put the current normalized spectral density S_I/I^2 in the range of 10^{-9}–$10^{-7}\,\mathrm{Hz}^{-1}$ at $f = 10\,\mathrm{Hz}$.[17] A more informative characteristic of 1/*f* noise level in two-dimensional (2D) materials is the noise spectral density normalized to the device channel area, which we denote as parameter $\beta = (S_I/I^2)(W \times L)$, where W is the channel width and L is the channel length. Independent studies established that β parameter is in the range from $\sim 10^{-8}$ to $10^{-7}\,\mu\mathrm{m}^2\ \mathrm{Hz}^{-1}$ for micrometer scale graphene devices on Si/SiO_2 substrate. Another important finding reported by several groups[17,19,28–30] was that 1/*f* noise in graphene does not follow the McWhorter model[32] conventionally used for description of noise in Si complementary metal-oxide-semiconductor (CMOS) transistors and field-effect transistors (FETs) made of other conventional semiconductors.[15]

Different mechanism of noise in graphene calls for investigation of the noise reduction techniques that can be effective for the specific material system. In this letter, we report on the low-frequency noise in the hexagonal boron nitride–graphene–boron nitride (*h*-BN-G-*h*-BN) heterostructure field-effect transistors (HFETs) on Si/SiO_2 substrates. The mobility in back- and top-gated graphene devices on Si/SiO_2 substrates used for noise studies previously was in the range from 1500 to 7000 cm^2/V s at room temperature (RT). In our HFETs, graphene channel is screened from defects by the hexagonal BN cap and barrier layers. The latter resulted

[a)]Author to whom correspondence should be addressed. Electronic mail: balandin@ee.ucr.edu

 © 2015 AIP Publishing LLC

This article is copyrighted as indicated in the article. Reuse of AIP content is subject to the terms at: http://scitation.aip.org/termsconditions. Downloaded to IP: 172.15.52.34 On: Tue, 14 Jul 2015 15:28:10

in RT mobility in the back-gated graphene HFETs in the range from ∼30 000 to 36 000 cm^2/Vs and allowed us to study the low-frequency noise in the supported graphene devices operating in the near-ballistic transport regime.[33]

The specific structure of *h*-BN-G-*h*-BN heterogeneous device channel was selected following the reports of mobility enhancement in graphene devices on *h*-BN substrate.[34–36] We modified the device design by using a thicker *h*-BN barrier and cap layers for better screening from the defects. Raman spectroscopy (Renishaw InVia) was used to determine the number of atomic planes in the exfoliated graphene samples and to verify the quality of the selected graphene and *h*-BN layers used for the device fabrication. The devices were fabricated in the following steps. First, *h*-BN layers (thickness $H \sim 30$ nm) were mechanically exfoliated on top of p-doped Si/SiO_2 wafer (300 nm of SiO_2). Graphene layers were prepared by the same procedure on another Si/SiO_2 substrate. Thin viscoelastic materials (Gelpak) adhered to glass slides were used as transparent stamps for the layer transfer. The stamps were spin-coated (Headway SCE) with polypropylene carbonate (PPC). Second, the stamp with PPC was brought into contact with the *h*-BN layer on a substrate using a micromanipulator. The stage was heated to 40 °C allowing for adherence of *h*-BN crystal with subsequent lifting of the stamp with attached *h*-BN layer. Third, the micromanipulator was used for careful positioning of *h*-BN layer over the graphene layer. Pressing the stamp with *h*-BN layer on top against monolayer graphene placed on a SiO_2 substrate and heating the stage to 40 °C led to the adherence of the graphene layer to *h*-BN. Repeating these steps, *h*-BN–graphene–*h*-BN stacks were formed creating the desired heterostructure. The completed heterostructure was released by heating the stage to 90 °C onto the degenerately doped p-type Si/SiO_2 substrate. Finally, the PPC layer was washed out with acetone to leave the assembled stack on the substrate. No cleaning treatments like thermal annealing have been used before and during the assembly process, as well as in the post-fabrication stage.

The fabricated heterostructures were spin coated and heated with a positive resist polymethyl methacrylate (PMMA) two times. Patterning of the assembled stacks was accomplished by electron beam lithography (EBL) (LEO Supra). In order to expose encapsulated graphene edges, the assembled stacks were selectively etched with sulfur hexafluoride (SF6) gas on an inductively coupled plasma system (Oxford Plasmalab) into conventional Hall bar geometries. The samples were rinsed with acetone to remove the resist mask. After the repeated PMMA spin coating procedures, the electrical contacts were patterned with EBL. Immediately before metallization, the graphene edges were exposed to O_2 plasma to improve bonding and increase transmission.[37,38] The metal leads (10 nm Cr/100 nm Au) were deposited by electron beam evaporation (Temescal BJD). The electrical contacts were made to Cr adhesion layers because the Cr work function is ∼0.16 eV lower than that of graphene.[39] The fabricated three-dimensional (3D) Cr/Au electrodes touched the 2D graphene monolayer along the one-dimensional (1D) graphene edge in these devices. This "1D contact" approach is typically advantageous in comparison to conventional "2D contacts" in the sense of separating the layer assembly and metallization processes, lower contact resistance.[38] The schematics and optical microscopy image of a representative device are presented in Figure 1. Total of eight devices were studied in this work.

Transport measurements were done in a two-probe configuration with the heavily doped Si substrate used as the back-gate. Figure 2 shows the current-voltage (I-V) characteristics of a representative *h*-BN-G-*h*-BN HFET with $L = 9.45\,\mu$m. The effective mobility, μ_{eff}, was determined from the channel resistance using the expression

$$\mu_{EFF} = \frac{L_G}{R_{EFF} C_G (V_{GS} - V_D) W}, \tag{1}$$

where L_G is the gate length, C_G is the gate capacitance per unit area, $R_{EFF} = \frac{R_{DS} - R_C}{1 - \sigma_0 (R_{DS} - R_C)}$, σ_0 is the conductivity at the voltage corresponding to the charge neutrality point, R_C is the sum of the drain and source contact resistances, and R_{DS} is the measured drain-source contact resistance. All our measurements were performed in the linear regime at very small currents so that the external V_{GS} was approximately equal to the intrinsic source-gate voltage. The field-effect mobility, μ_{FE}, was determined from the transconductance, g_{m0}, in the linear regime using the expression

$$\mu_{FE} = \frac{g_{m0}}{C_G (V_{DS} - I R_C)} \frac{L_G}{W}, \tag{2}$$

where V_{DS} is the drain-source voltage. In the linear regime at small drain voltages, the internal transconductance was found from

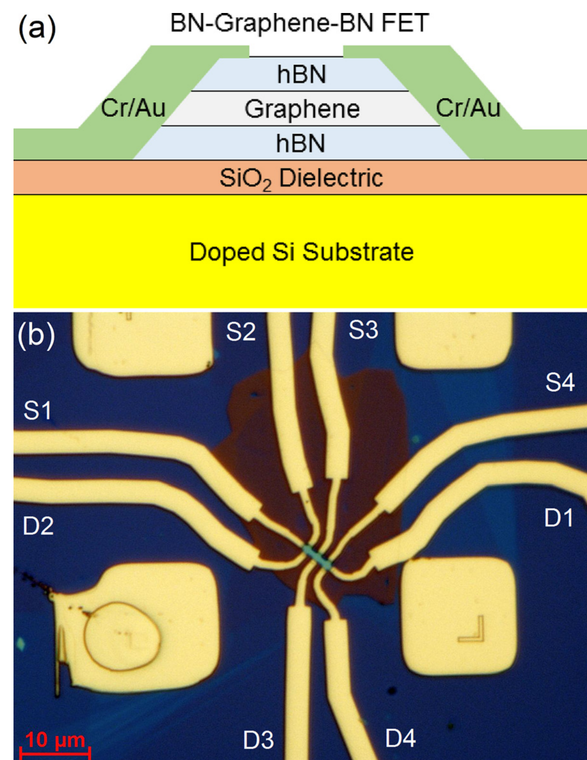

FIG. 1. (a) Schematics of *h*-BN-G-*h*-BN HFET. Note the structure the "one-dimensional" contact to the fully encapsulated graphene layer. (b) Optical microscopy image of a representative graphene encapsulated HFET. The source and drain contacts of the device are denoted with S and D symbols, respectively.

This article is copyrighted as indicated in the article. Reuse of AIP content is subject to the terms at: http://scitation.aip.org/termsconditions. Downloaded to IP: 172.15.52.34 On: Tue, 14 Jul 2015 15:28:10

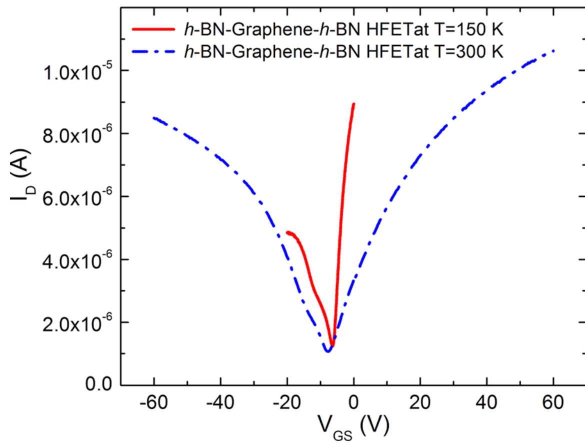

FIG. 2. Current–voltage transfer characteristics of *h*-BN-G-*h*-BN HFETs. The source-drain voltage is 10 mV.

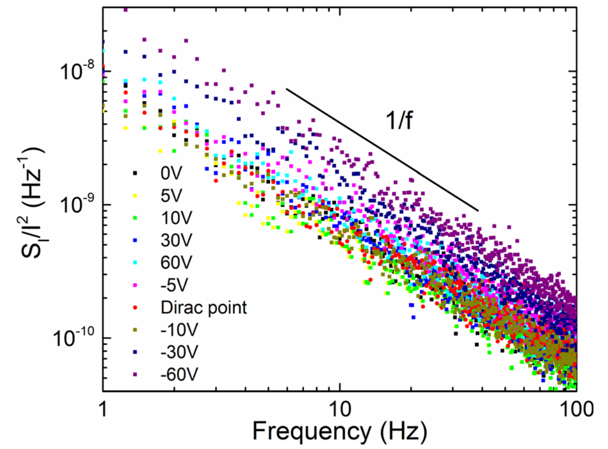

FIG. 3. Normalized noise spectrum density in *h*-BN-G-*h*-BN HFET as a function of frequency for several values of the back-gate bias V_G. Note that $V_G = -7.75$ V corresponds to the Dirac point.

$$g_{m0} \approx g_m\left(1 + \frac{R_C}{R_{EFF}} + R_C\sigma_0\right), \quad (3)$$

where g_m is the external transconductance. Both the effective and field-effect mobility extractions gave consistent results, and the charge carrier mobility was determined to be greater than 30 000 cm^2/Vs at RT and for the carrier concentration of 7×10^{11} cm^{-2}. The low-temperature ($T = 77$ K) mobility values reached 100 000 cm^2/Vs.

An estimate for the contact resistance, R_C, was obtained by plotting the drain-to-source resistance, R_{DS}, versus $1/(V_G - V_D)$, where V_G is the gate bias and V_D is the Dirac (charge-neutrality point) voltage. An extrapolation of this dependence to $1/(V_G - V_D) = 0$ provides the sum of the drain and source contact resistance R_C. For the studied devices, the value of the contact resistance per unit width $R_{c0} = R_C \times W/2$ was $\sim 277\ \Omega\,\mu$m. To estimate the charge carrier mean free path (MFP), Λ, we used a conventional relation between the mobility, μ, and electrical conductivity $\sigma = en\mu = (2e^2/h)k_F\Lambda$, where $k_F = (\pi n)^{1/2}$ is the Fermi wave vector in 2D graphene, h is the Planck's constant, e is the charge of an electron, and n is the carrier concentration. For $n = 2 \times 10^{12}$ cm^{-2}, from the expression $\Lambda = (h/2e)\mu(n/\pi)^{1/2}$ we obtained $\Lambda \approx 0.311\ \mu$m. For devices with $W \approx 1\ \mu$m and L in the range from 2.5 to 9.45 μm, the electron transport is not yet ballistic, but it approaches this regime. As predicted in Ref. 40, the unique features of the near ballistic response could be revealed by studying "ringing" of the transistor response to short THz pulses.

The low-frequency noise was measured using an in-house built experimental setup with a spectrum analyzer (SRS FFT). The devices were biased with a "quiet" battery–-potentiometer circuit. Details of our noise measurement procedures have been reported by some of us elsewhere.[18,19,22] Figure 3 shows representative normalized noise spectrum density, S_I/I^2, for one of the tested devices. The noise is of true $1/f^\gamma$ type with γ varying from 0.95 to 1.2 with an average $\gamma = 1.09$ for a device with the channel $W \times L = 1.16 \times 9.45\ \mu$m^2. For the device with the channel $W \times L = 1 \times 3.21\ \mu$m^2, the extracted γ was in the range from 0.84 to 1.27 with an average value of $\gamma = 1.02$. Table I lists the γ values for two representative devices. No trend in γ dependence with the device channel area or gate voltage, which would suggest non-uniformity of the charge trap distribution,[15] was observed. The noise spectra of all examined devices revealed no traces of the generation-recombination noise. The noise spectrum density of the high-mobility *h*-BN-G-*h*-BN HFETs revealed strongly non-monotonic gate-bias dependence, which is in contrast to that described by the McWhorter model in Si CMOS devices.[32]

To better elucidate the non-monotonic type of the noise gate bias dependence we calculated the noise amplitude as $A = \frac{1}{Z}\sum_{i=1}^{Z} f_i S_{Ii}/I^2$, which is a dimensionless noise characteristic analogous to the normalized noise spectral density S_I/I^2 but averaged over several frequencies (here Z is the number of the frequency data points). Figure 4(a) shows the noise amplitude in our *h*-BN-G-*h*-BN HFET as a function of V_{GS}-V_D (V_D is the Dirac voltage). For comparison, we also show noise amplitude in conventional non-encased graphene FET on Si/SiO$_2$ reported in Ref. 28. The non-encased graphene FET had mobility less than 3000 cm^2/Vs. In our high-mobility *h*-BN-G-*h*-BN HFETs, the minimum of the noise amplitude was achieved near the Dirac point, similar to that in the conventional graphene FETs.[17,28] The McWhorter model predicts that S_I/I^2 decreases in the inversion regime as $\sim(1/n)^2$. In graphene FETs on Si/SiO$_2$, the noise gate dependence has characteristic "M" shape.[17] The noise gate dependence in our h-BN-G-h-BN HFETs is also close to "M" shape and it does not follow the McWhorter model.

The parameter $\beta = (S_I/I^2)(W \times L)$ is a better characteristic of 1/*f* noise in 2D materials than Hooge parameter introduced specifically for volume noise.[22] For conventional graphene devices on Si/SiO$_2$ substrates, β parameter is $\sim 10^{-8}$ to $10^{-7}\ \mu$m^2 Hz^{-1} for micrometer-scale channels.[17] In our high-mobility *h*-BN-G-*h*-BN HFETs, β was determined to be in the range from 5×10^{-9} to $2 \times 10^{-8}\ \mu$m^2

TABLE I. Parameter γ for low-frequency noise in BN-graphene-BN HFETs.

V_G (V)	−60	−30	−10	−8	−5	0	5	10	30	60
γ (device A)	1.16	1.04	0.96	1.19	0.95	1.16	0.97	1.12	1.12	1.20
γ (device B)	1.27	0.84	0.95	1.04	1.02	1.02	0.96	0.94	1.04	1.05

This article is copyrighted as indicated in the article. Reuse of AIP content is subject to the terms at: http://scitation.aip.org/termsconditions. Downloaded to IP: 172.15.52.34 On: Tue, 14 Jul 2015 15:28:10

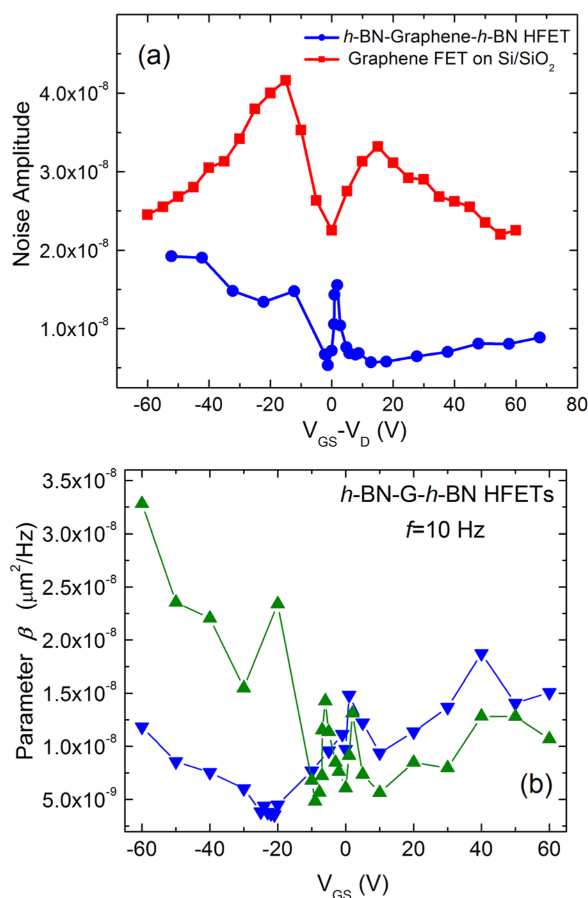

FIG. 4. (a) Noise amplitude as a function of the gate bias with respect to the Dirac point, V_{GS}-V_D for *h*-BN-G-*h*-BN HFET. The results are shown for the device with the largest channel dimensions. The data for conventional non-encapsulated graphene FET on Si/SiO$_2$ wafer from Ref. 28 are also shown for comparison. (b) Parameter β, which defines 1/*f* noise level in 2D channels plotted as a function of gate bias for two representative devices.

Hz^{-1}. At small gate biases the noise level was typically below 10^{-8} μm^2 Hz^{-1} in *h*-BN-G-*h*-BN HFETs. Figure 4(b) shows parameter β dependence on the gate bias for two representative devices. On average, 1/*f* noise in our devices was suppressed by a factor of $\times 5 - \times 10$ as compared to that in non-encapsulated graphene devices on Si/SiO$_2$. This is a substantial reduction, which can have practical implications.

We now turn to explanation of a potential mechanism of noise reduction in encased graphene channel devices. It is generally accepted now that the low frequency 1/*f* noise can be either due to the number of charge carrier fluctuations or due to their mobility fluctuations or both. Depending on which term dominates, one distinguishes the mobility fluctuation or the carrier number fluctuation mechanism of 1/*f* noise.[15] In Si and other metal-oxide-semiconductor field-effect transistors (MOSFETs), the carrier number fluctuations usually dominate and such type of the noise is well described by the McWhorter model.[32] The studies that investigate noise in graphene under irradiation[19] and magnetic field[41] suggested that the mechanism of 1/*f* noise in graphene is more similar to the mobility fluctuations mechanism (like that in metals).

Owing to graphene's atomic thickness and the fact the mobility is limited by scattering from defects and impurities in SiO$_2$,[42–46] the mobility fluctuations will be due to the fluctuations in the scattering cross-sections of defect states in SiO$_2$ gate dielectric. For this reason, irrespective of the specific noise mechanism—carrier number or mobility fluctuations—screening electrons in graphene channel from the defect states in SiO$_2$ by introducing *h*-BN barrier layer with the thickness of 30 nm should reduce the noise. This conclusion is consistent with reports that 1/*f* noise was reduced in the suspended graphene devices.[23] It is interesting to note that suspended graphene device reported in Ref. [23] had $\beta \sim 6 \times 10^{-9}$ μm^2/Hz, which is approximately the same noise level as in our encased graphene channel HFETs. While most of noise reduction is likely related to screening of the graphene channel from traps in SiO$_2$, it is possible that capping graphene with *h*-BN also helps to reduce the noise. It has been shown that the environmental exposure and device ageing increase the level of 1/*f* noise in graphene devices.[17,22] Organic residue and other contaminants on the surface can create either trapping centers for electrons in the channel (carrier number fluctuation noise) or scattering centers (mobility fluctuation noise).

In conclusion, we investigated the low-frequency 1/*f* noise in the *h*-BN-graphene-*h*-BN HFETs with mobility in the range from 30 000 to 36 000 cm^2/Vs. It was established that 1/*f* noise in such device is strongly suppressed as compared to that in non-encapsulated graphene devices on Si/SiO$_2$. Considering that *h*-BN is chemically stable and produces strong positive effect on mobility in graphene channel, our finding that the *h*-BN capping and barrier layers result in significant reduction of 1/*f* noise adds an extra merit to practical electronic applications of graphene-based heterostructures.

The work at UC Riverside was supported, in part, by the Semiconductor Research Corporation (SRC) and Defense Advanced Research Project Agency (DARPA) through STARnet Center for Function Accelerated nanoMaterial Engineering (FAME) and by the National Science Foundation (NSF) project Graphene Circuits for Analog, Mixed-Signal, and RF Applications (NSF CCF-1217382). S.L.R. acknowledges partial support from the Russian Fund for Basic Research (RFBR). The work at RPI was supported by the Army Research Office (Program Manager: Dr. Meredith Reed).

[1] A. K. Geim and K. S. Novoselov, "The rise of grapheme," Nat. Mater. **6**(3), 183–191 (2007).
[2] A. V. Kretinin, Y. Cao, J. S. Tu, G. L. Yu, R. Jalil, K. S. Novoselov, S. J. Haigh, A. Gholinia, A. Mishchenko, M. Lozada, T. Georgiou, C. R. Woods, F. Withers, P. Blake, G. Eda, A. Wirsig, C. Hucho, K. Watanabe, T. Taniguchi, A. K. Geim, and R. V. Gorbachev, "Electronic properties of graphene encapsulated with different two-dimensional atomic crystals," Nano Lett. **14**(6), 3270–3276 (2014).
[3] G. X. Liu, S. Ahsan, A. G. Khitun, R. K. Lake, and A. A. Balandin, "Graphene-based non-Boolean logic circuits," J. Appl. Phys. **114**(15), 154310 (2013).
[4] X. B. Yang, G. X. Liu, A. A. Balandin, and K. Mohanram, "Triple-mode single-transistor graphene amplifier and its applications," ACS Nano **4**(10), 5532–5538 (2010).
[5] X. B. Yang, G. X. Liu, M. Rostami, A. A. Balandin, and K. Mohanram, "Graphene ambipolar multiplier phase detector," IEEE Electron Device Lett. **32**(10), 1328–1330 (2011).
[6] F. Schwierz, "Graphene transistors," Nat. Nanotechnol. **5**(7), 487–496 (2010).

This article is copyrighted as indicated in the article. Reuse of AIP content is subject to the terms at: http://scitation.aip.org/termsconditions. Downloaded to IP: 172.15.52.34 On: Tue, 14 Jul 2015 15:28:10

[7]L. Liao, Y. C. Lin, M. Q. Bao, R. Cheng, J. W. Bai, Y. A. Liu, Y. Q. Qu, K. L. Wang, Y. Huang, and X. F. Duan, "High-speed graphene transistors with a self-aligned nanowire gate," Nature **467**(7313), 305–308 (2010).
[8]T. Otsuji, A. Satou, T. Watanabe, A. Dubinov, V. Popov, S. A. B. Tombet, V. Mitin, and V. Ryzhii, "Graphene active plasmonics and their applications to terahertz lasers and sensors," Proc. SPIE **8993**, 899327 (2014).
[9]T. Otsuji, A. Satou, T. Watanabe, S. A. Boubanga-Tombet, M. Ryzhii, A. Dubinov, V. V. Popov, V. Mitin, M. Shur, and V. Ryzhii, "Recent advances in the research toward graphene-based terahertz lasers," Proc. SPIE **9382**, 938219 (2015).
[10]F. Schedin, A. K. Geim, S. V. Morozov, E. W. Hill, P. Blake, M. I. Katsnelson, and K. S. Novoselov, "Detection of individual gas molecules adsorbed on graphene," Nat. Mater. **6**(9), 652–655 (2007).
[11]S. Rumyantsev, G. X. Liu, M. S. Shur, R. A. Potyrailo, and A. A. Balandin, "Selective gas sensing with a single pristine graphene transistor," Nano Lett. **12**(5), 2294–2298 (2012).
[12]S. Rumyantsev, G. X. Liu, R. A. Potyrailo, A. A. Balandin, and M. S. Shur, "Selective sensing of individual gases using graphene devices," IEEE Sens. J. **13**(8), 2818–2822 (2013).
[13]R. Samnakay, C. Jiang, S. L. Rumyantsev, M. S. Shur, and A. A. Balandin, "Selective chemical vapor sensing with few-layer MoS2 thin-film transistors: Comparison with graphene devices," Appl. Phys. Lett. **106**(2), 023115 (2015).
[14]R. Pettai, *Noise in Receiving Systems* (Wiley, 1984).
[15]A. A. Balandin, *Noise and Fluctuation Control in Electronic Devices* (American Scientific Publishers, Los Angeles, 2002).
[16]R. A. Potyrailo, C. Surman, N. Nagraj, and A. Burns, "Materials and transducers toward selective wireless gas sensing," Chem. Rev. **111**(11), 7315–7354 (2011).
[17]A. A. Balandin, "Low-frequency 1/f noise in graphene devices," Nat. Nanotechnol. **8**(8), 549–555 (2013).
[18]G. X. Liu, S. Rumyantsev, M. S. Shur, and A. A. Balandin, "Origin of 1/f noise in graphene multilayers: Surface vs. volume," Appl. Phys. Lett. **102**(9), 093111 (2013).
[19]M. Z. Hossain, S. Rumyantsev, M. S. Shur, and A. A. Balandin, "Reduction of 1/f noise in graphene after electron-beam irradiation," Appl. Phys. Lett. **102**(15), 153512 (2013).
[20]Y. M. Lin and P. Avouris, "Strong suppression of electrical noise in bilayer graphene nanodevices," Nano Lett. **8**(8), 2119–2125 (2008).
[21]Q. H. Shao, G. X. Liu, D. Teweldebrhan, A. A. Balandin, S. Runryantsev, M. S. Shur, and D. Yan, "Flicker noise in bilayer graphene transistors," IEEE Electron Device Lett. **30**(3), 288–290 (2009).
[22]S. Rumyantsev, G. Liu, W. Stillman, M. Shur, and A. A. Balandin, "Electrical and noise characteristics of graphene field-effect transistors: ambient effects, noise sources and physical mechanisms," J. Phys. Condens. Matter **22**(39), 395302 (2010).
[23]Z. G. Cheng, Q. Li, Z. J. Li, Q. Y. Zhou, and Y. Fang, "Suspended graphene sensors with improved signal and reduced noise," Nano Lett. **10**(5), 1864–1868 (2010).
[24]I. Heller, S. Chatoor, J. Mannik, M. A. G. Zevenbergen, J. B. Oostinga, A. F. Morpurgo, C. Dekker, and S. G. Lemay, "Charge noise in graphene transistors," Nano Lett. **10**(5), 1563–1567 (2010).
[25]S. A. Imam, S. Sabri, and T. Szkopek, "Low-frequency noise and hysteresis in graphene field-effect transistors on oxide," Micro Nano Lett. **5**(1), 37–41 (2010).
[26]G. Liu, W. Stillman, S. Rumyantsev, Q. Shao, M. Shur, and A. A. Balandin, "Low-frequency electronic noise in the double-gate single-layer graphene transistors," Appl. Phys. Lett. **95**(3), 033103 (2009).
[27]A. N. Pal and A. Ghosh, "Ultralow noise field-effect transistor from multilayer graphene," Appl. Phys. Lett. **95**(8), 082105 (2009).
[28]G. Y. Xu, C. M. Torres, Y. G. Zhang, F. Liu, E. B. Song, M. S. Wang, Y. Zhou, C. F. Zeng, and K. L. Wang, "Effect of spatial charge inhomogeneity on 1/f noise behavior in Graphene," Nano Lett. **10**(9), 3312–3317 (2010).
[29]Y. Zhang, E. E. Mendez, and X. Du, "Mobility-dependent low-frequency noise in graphene field-effect transistors," ACS Nano **5**(10), 8124–8130 (2011).
[30]A. A. Kaverzin, A. S. Mayorov, A. Shytov, and D. W. Horsell, "Impurities as a source of 1/f noise in grapheme," Phys. Rev. B **85**(7), 075435 (2012).
[31]P. Dutta and P. M. Horn, "Low-frequency fluctuations in solids - 1-F noise," Rev. Mod. Phys. **53**(3), 497–516 (1981).
[32]A. L. McWhorter and R. H. Kingston, *Semiconductor Surface Physics* (University of Pennsylvania Press, 1957).
[33]M. S. Shur and L. F. Eastman, "Ballistic and near ballistic transport in GaAs," Electron Device Lett. **1**(8), 147–148 (1980).
[34]C. R. Dean, A. F. Young, I. Meric, C. Lee, L. Wang, S. Sorgenfrei, K. Watanabe, T. Taniguchi, P. Kim, K. L. Shepard, and J. Hone, "Boron nitride substrates for high-quality graphene electronics," Nat. Nanotechnol. **5**(10), 722–726 (2010).
[35]A. S. Mayorov, R. V. Gorbachev, S. V. Morozov, L. Britnell, R. Jalil, L. A. Ponomarenko, P. Blake, K. S. Novoselov, K. Watanabe, T. Taniguchi, and A. K. Geim, "Micrometer-scale ballistic transport in encapsulated graphene at room temperature," Nano Lett. **11**(6), 2396–2399 (2011).
[36]A. K. Geim and I. V. Grigorieva, "Van der Waals heterostructures," Nature **499**(7459), 419–425 (2013).
[37]Y. Matsuda, W. Q . Deng, and W. A. Goddard, "Contact resistance for "end-contacted" metal-graphene and metal-nanotube interfaces from quantum mechanics," J. Phys. Chem. C **114**(41), 17845–17850 (2010).
[38]L. Wang, I. Meric, P. Y. Huang, Q. Gao, Y. Gao, H. Tran, T. Taniguchi, K. Watanabe, L. M. Campos, D. A. Muller, J. Guo, P. Kim, J. Hone, K. L. Shepard, and C. R. Dean, "One-dimensional electrical contact to a two-dimensional material," Science **342**(6158), 614–617 (2013).
[39]G. Giovannetti, P. A. Khomyakov, G. Brocks, V. M. Karpan, J. van den Brink, and P. J. Kelly, "Doping graphene with metal contacts," Phys. Rev. Lett. **101**(2), 026803 (2008).
[40]S. Rudin, R. G. Rupper, and M. Shur, "Ultimate response time of high electron mobility transistors," J. Appl. Phys. **117**, 174502 (2015).
[41]S. L. Rumyantsev, D. Coquillat, R. Ribeiro, M. Goiran, W. Knap, M. S. Shur, A. A. Balandin, and M. E. Levinshtein, "The effect of a transverse magnetic field on 1/f noise in graphene," Appl. Phys. Lett. **103**(17), 173114 (2013).
[42]T. Ando, "Screening effect and impurity scattering in monolayer graphene," J. Phys. Soc. Jpn. **75**(7), 074716 (2006).
[43]J. H. Chen, C. Jang, S. D. Xiao, M. Ishigami, and M. S. Fuhrer, "Intrinsic and extrinsic performance limits of graphene devices on SiO_2," Nat. Nanotechnol. **3**(4), 206–209 (2008).
[44]E. H. Hwang, S. Adam, and S. Das Sarma, "Carrier transport in two-dimensional graphene layers," Phys. Rev. Lett. **98**(18), 186806 (2007).
[45]K. Nomura and A. H. MacDonald, "Quantum transport of massless dirac fermions," Phys. Rev. Lett. **98**(7), 076602 (2007).
[46]S. Fratini and F. Guinea, "Substrate-limited electron dynamics in graphene," Phys. Rev. B **77**(19), 195415 (2008).

This article is copyrighted as indicated in the article. Reuse of AIP content is subject to the terms at: http://scitation.aip.org/termsconditions. Downloaded to IP: 172.15.52.34 On: Tue, 14 Jul 2015 15:28:10